[15] Clarkson, R. E., Field, R. E., Jr., and Keefer, D. R., "Electron Temperatures in Several rf General Plasmas," *AIAA Journal*, Vol. 4, No. 3, March 1966, pp. 546–547.

[16] Seemann, G. R., Thornton, J. A., and Penfold, A. S., "Experimental Study of a Traveling Wave Accelerator," *AIAA Journal*, Vol. 4, No. 10, Oct. 1966, pp. 1870–1872.

[17] Seemann, G. R., Penfold, A. S., and Thornton, J. A., "The Minimum Specific Energy and Electric Field Necessary to Sustain a Flowing Induction Plasma," *Journal of Applied Physics*, Vol. 39, No. 1, Jan. 1968, pp. 340–342.

[18] Seemann, G. R., Thornton, J. A., and Penfold, A. S., "Subsonic Plasma Tunnel for Evaluating Re-Entry Flight Instrumentation," *AIAA Journal*, Vol. 6, No. 8, Aug. 1968, pp. 1592–1594.

[19] Seemann, G. R. and Thornton, J. A., "Experimental Investigation of a Flush Electrostatic Double Probe for Re-Entry Measurements," AIAA Paper 69-700, San Francisco, Calif., 1969.

[20] Warder, R. C., Jr. and Thornton, J. A., "An Experimental Study of the Breakdown Characteristics of Microwave and VHF Antennas, Vol. 1," AFCRL-68-0450, July 1968, Air Force Cambridge Research Lab., Cambridge, Mass.

JUNE 1970 AIAA JOURNAL VOL. 8, NO. 6

Effect of Mass Injection on a High-Current Arc

RODNEY L. BURTON,* PIERRE DEVILLERS,† AND ORSON CHANG†
University of California, San Diego, La Jolla, Calif.

To understand better the MPD arc and other accelerating high-current arcs, experimental and theoretical investigations are presented for a parallel-plate quasi-steady arc with argon or helium injection from a linear slit at the midplane. The arc is quasi-steady for about 350 μsec, and the quasi-steady current is 4–14 ka. Mass flow rate is set and controlled by an electromagnetically driven gas valve. It is found that at low mass flow rate the arc inductance oscillates, but that at a sufficiently high mass flow rate $\dot{m}_c$, the arc voltage becomes constant. Measurements of $\dot{m}_c$ in argon and helium show a dependence $\dot{m}_c \sim I^2/u_c$, where $u_c = (2eV_i/m)^{1/2}$ is the critical speed corresponding to the ionization potential. In addition, arc voltage is found to increase linearly with current. A simplified theoretical model is developed, based on one-dimensional constant area flow of a monofluid. Two physical constraints must be imposed to determine the downstream flow conditions, and these are 1) sonic downstream flow, and 2) $\dot{m}$ adjusts to minimize arc power input. These constraints predict $\dot{m} \sim I^2/u_c$, and an electrical impedance $Z \sim u_c$. Both of these results show reasonable agreement with experiment. Application of the theory to high-current arcs with no mass injection indicates that the electrodes erode at a rate proportional to I^2.

I. Introduction

ONE of the most intriguing questions to be asked about accelerating arc discharges is that of how the arc utilizes the mass flow available to it. An early and most celebrated fact about the MPD arc was its ability to produce thrust with no input mass flow,[1] due to the utilization of background mass and/or electrode material. It has also been observed[2–5] that the arc parameters of thrust and voltage are independent of the mass flow rate over a wide range. This behavior suggests that the MPD arc in some manner adjusts the amount of mass to be accelerated, independently of the mass fed into it, and mechanisms for this adjustment have been proposed by Cann,[6] Bennett et al.,[3] and Stratton.[7]

In this paper some experiments on quasi-steady parallel-plate arcs will be described, and the results will be compared with previous theory and with a one-dimensional arc model.

Presented as Paper 69–266 at the AIAA 7th Electric Propulsion Conference, Williamsburg, Va., March 3–5, 1969; submitted July 22, 1969; revision received December 29, 1969. This research was supported by the Advanced Research Projects Agency of the Department of Defense and was monitored by the U. S. Army Research Office-Durham under Contract DA-31-124-ARO-D-257. The authors are indebted to W. A. Conner for the construction of the apparatus, and to J. C. Sherman for his critical comments on the paper.

* Assistant Professor of Engineering Physics, Department of Aerospace and Mechanical Engineering Sciences. Member AIAA.

† Graduate Student, Department of Aerospace and Mechanical Engineering Sciences.

II. Previous Experiments

In previously reported work[8] it was demonstrated that an arc current of up to 50 ka in a parallel-plate accelerator could be stabilized by partially insulating the electrodes. This result has also been achieved by Eckbreth and Jahn.[9] The arc chamber, shown in Fig. 1, is rectangular with internal dimensions 10 × 10 × 25 cm. The chamber is filled with argon at a pressure of 0.075–0.60 torr, and the electrodes are driven by a 35 μsec flat-topped pulse of current, of 25–50 ka. With magnetic probe coils (Fig. 1), it was demonstrated that after a short transient phase, the magnetic field pattern becomes nearly steady. In addition, the voltages V_0 and V_{28} are equal in steady operation (Fig. 1), so that the magnetic flux threading the electrodes between the probes is a constant. Since the magnetic pressure behind the sheet at 50 ka is 1.4 atm, the fluid is pumped in the positive x direction.

It was clear from the results that this arc, operating with no mass injection, primarily accelerates electrode material. Severe pitting occurs in the brass electrodes, although not in the nylon insulator, and electrode material is plated onto the downstream endwall. It is calculated that the argon fill available to the arc is depleted during the time of the discharge, assuming that the argon is fully ionized and that the argon energy is on the order of the ionization potential. This view is also supported by Kerr Cell photographs of the discharge, showing that the plasma is only luminous near the electrodes.

For future comparison with the mass-injected arc, which does not run on electrode material, it will be useful to summarize the results of terminal and internal measurements for the case of no mass injection; 1) arc voltage is independent

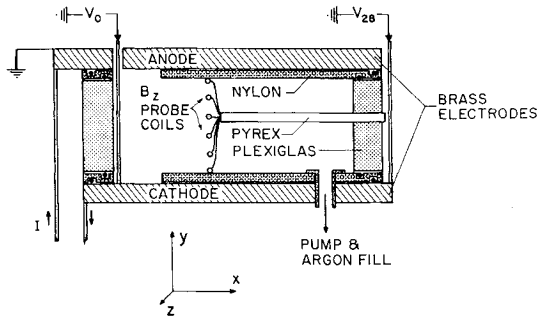

Fig. 1 Schematic of parallel-plate accelerator with partially insulated electrodes and no mass injection.

of argon fill pressure, apparently because the arc runs on electrode material, 2) arc voltage is 750 v at 50 ka and 400 v at 25 ka, implying an arc impedance of 14 mΩ, and 3) the arc inductance is ~0.13 μh, corresponding to a 4 cm excursion of the magnetic field pattern downstream from the edge of the insulator (Fig. 2).

III. Present Experiments

In the present experiments the rectangular electrode geometry has been retained (Fig. 3). The arc discharges into a 1 m³ tank, and the electrode spacing is reduced to 3.75 cm. Electrode length in the z direction perpendicular to Fig. 3 is 8.2 cm and in the flow direction is 1.0 cm. The electrodes are Elkonite, a 57% W, 43% Cu alloy, and are capped with nylon insulators to simulate the previous arc geometry. There are no sidewalls. Argon or helium is injected through an adjustable width slit midway between the electrodes.

Fast Gas Valve

In order to initiate gas injection on a time scale short compared to the duration of the driving current pulse, a conventional[10] electromagnetically driven gas valve is incorporated into the arc (Fig. 3). The valve coil has an inductance of 0.3 μh, and is driven by a 33 μfd low inductance capacitor charged to 4 kv. When a series spark gap is fired, the circuit rings down at 50 kHz, driving 42 ka through the coil. This current induces an eddy current in an aluminum disk, which is attached to a shaft, and thence to a valve plate which acts as an O-ring surface. By measuring the time required for the plate to pass through a 1 mm diam laser beam, it is found that the plate executes elastic oscillations on the end of the shaft connecting it to the aluminum disk, and simultaneously accelerates to an average velocity $\dot{x}$ of ~1.7 m/sec within about 10 μsec. Thus, for a typical width setting of the injection slit at 0.25 mm, the slit is effectively opened in ~75 μsec.

The slit opening time is thus short compared to the gas flow rise time into the device. Unfortunately, attempts to measure flow times with a fast ionization gage met with failure, apparently because of the relatively high (~10^{-3} torr) background pressure in the tank which poisoned the miniature pentode (CK5702). Attempts to avoid cathode poisoning by constructing a miniature guillotine to break the tube's glass envelope in vacuum proved fruitless.

We must therefore be satisfied with an estimate of the flow rate rise time. The sonic time from the O-ring to the slit, plus the supersonic flight time from slit to electrode, is calculated to be ~50 μsec, comparable to the valve opening time. Much longer, however, is the time t_f required to fill the volume V of ~3 cm³ that exists between the O-ring and the slit. Assuming choked flow, and assuming that the plate moves at constant velocity away from the O-ring, then the number of particles N in the volume V will be proportional to t_f^2. Equating the particle density N/V with the plenum particle density gives the approximate formula

$$t_f^2 \approx (V/ba_0\dot{x}) \tag{1}$$

where b is the plate length perpendicular to the plane of Fig. 3, a_0 is the sound speed, and $\dot{x}$ is the average plate velocity discussed above. Equation (1) then gives $t_f \sim 300$ μsec for argon, and it is thus assumed that steady mass flow is achieved 300 μsec after firing the gas valve spark gap.

Since the arc breakdown is initiated by the fast gas valve, no other switch is incorporated into the arc circuit. It is found that for a typical mass flow, and gap voltage of 1 kv, the arc switches on reproducibly at 180 ± 20 μsec after the firing of the fast gas valve spark gap. At 1.4 kv or at high mass flow, this figure reduces to 140 ± 10 μsec, and at 0.4 kv and low mass flow rates is as high as 300 ± 20 μsec. The shot-to-shot reproducibility is therefore quite adequate (Fig. 4).

Once steady flow has been established, the mass flow is estimated using the standard isentropic equation for choked flow, multiplied by a discharge coefficient C_W for a typical Reynolds number of 10^4

$$\dot{m} = C_W \gamma p_0 A (2/\gamma + 1)^{(\gamma+1)/2(\gamma-1)}/a_0 \tag{2}$$

where p_0 and a_0 are stagnation pressure and sound speed, and A is the slit area. Equation (2) has been used to calculate the arc mass flow in Fig. 6 for $C_W = 0.5$, but because C_W and A are not known precisely, $\dot{m}$ is known only to within ±50%.

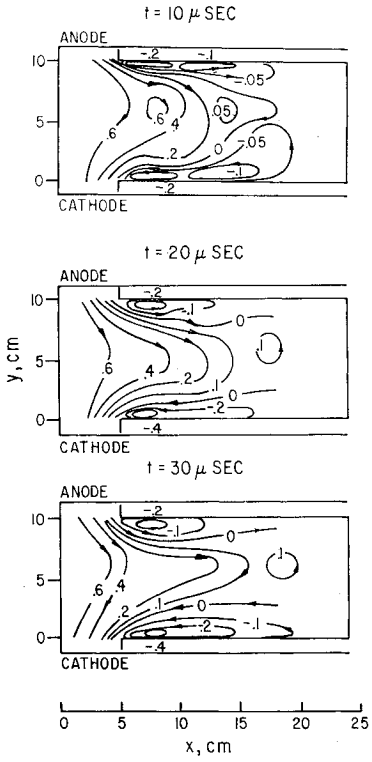

Fig. 2 Constant B_z contours (w/m^2) for parallel-plate accelerator with partially insulated electrodes and no mass injection. Arrows show the direction of current flow.

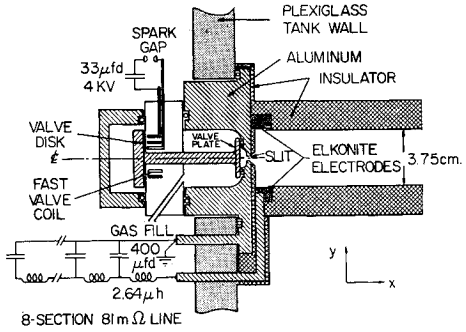

Fig. 3 Schematic of parallel-plate accelerator and mass injection system.

Transmission Line

The arc electrodes are connected through low-inductance parallel plates directly to an 8-section transmission line of standard design.[11] The 8×400 μfd capacitors are connected in series to three-turn 2.64 μh coils (Fig. 3), giving a line impedance Z_L of 81 mΩ. The line impedance is much larger than the arc impedance, so that the quasi-steady value of current I is very nearly given by line voltage divided by the line impedance of 81 mΩ. The current rises in 80 μsec to its quasi-steady value, and stays constant for 350 μsec before it begins to decrease.

Influence of Background Pressure

The tank is pumped by a Welch mechanical pump, and the best available vacuum is $\sim 10^{-3}$ torr. Since the transmission line voltage appears across the electrodes during the charging process, it is necessary to keep the background pressure below 5×10^{-3} torr to prevent arc breakdown. It is not expected that the background pressure has any influence on the quasi-steady running of the arc. The amount of mass injected during the first current pulse is enough to raise the background pressure by only 3-7 $\times 10^{-3}$ torr, and because the one-way transit time in the tank is $\sim$3 msec, the bulk of this mass will be at the far end of the tank away from the electrodes.

Firing Sequence

The sequence of events can therefore be reconstructed. At $t = 0$ the fast gas valve fires, initiating a constant velocity in the valve plate. At $t \approx 180$ μsec the discharge begins, and the current begins to rise. At $t \approx 260$ μsec the driving current reaches its quasi-steady value, and at $t \approx 300$ μsec (for argon, 170 μsec for helium), steady mass flow is established. The driving current then remains constant until $t \approx 610$ μsec, when it begins to reverse, and passes through zero at $t \approx 700$ μsec.

Measurements

A voltage-current survey was first taken for a range of mass flow rates in argon. The gas valve slit widths were 0.05, 0.125, 0.25, and 0.63 mm, and the plenum pressure was 25–65 psi, giving a mass flow between 0.6 and 16 g/sec. A typical oscillograph is shown in Fig. 4, in which the voltage across the electrodes is recorded vs time. Considering the uppermost set of traces in Fig. 4 ($\dot{m} = 14$ g/sec), the following sequence of events is observed. At $t = 0$ the fast gas valve fires, followed at $t = 150$ μsec by the initiation of the discharge. After a

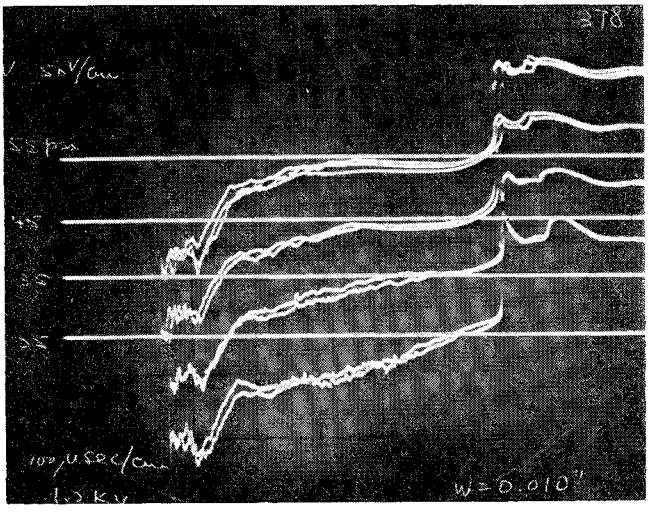

Fig. 4 Multiple overlay traces of arc voltage vs time at I = 14.2 ka, and four plenum pressures. Injected $\dot{m}$ varies from 6.5 to 14 g/sec argon.

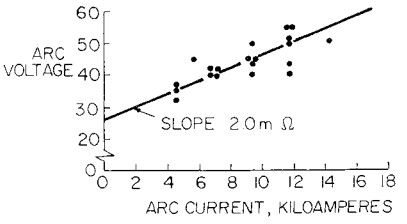

Fig. 5 Arc voltage vs current for argon flow rate $\dot{m} = \dot{m}_c$, the mass flow rate at which arc voltage is constant. Arc impedance is on the order of 2 mΩ.

transient period of some 50 μsec, while the voltage undergoes rapid oscillations, the voltage decreases slowly for $\sim$200 μsec to a constant value, which is held until current reversal begins. Then at $t = 700$ μsec the voltage changes sign, going from negative to positive in less than 10 μsec. Because the voltage reverses in 10 μsec compared to some 160 μsec for the current, it is concluded that voltage is essentially independent of current.

The measured voltage-current plot is shown in Fig. 5, for arc currents between 4.5 and 14.2 ka. To avoid errors due to shifts in ground potential, the voltage plotted is the average magnitude for the first and second current pulses. Points are taken only for times where V and I are constant. The arc voltage increases with current, and for $V(t) =$ constant can be approximated by the relation

$$V = V_0 + IZ \tag{3}$$

As shown in Fig. 5, Z has a value of 2 mΩ for argon, although the scatter in the data is such that this value is good to about ± 1 mΩ.

The effect of mass injection is shown clearly in Fig. 4, in which $\dot{m}$ varies from 6.5 g/sec for the lowest set of traces up to 14 g/sec for the uppermost set. At the low mass flow rate the voltage never becomes constant. Since the arc impedance is so low and current is constant, this decrease in arc voltage can best be explained by an $I\dot{L}$ effect, in which L is decreasing. This phenomena of decreasing inductance has been observed previously,[8,9] and occurs because the magnetic field pattern first blows out into the chamber after breakdown, and then slowly sags back (Fig. 2). The inductance thus quickly increases to a maximum after breakdown and then slowly decreases to a low inductance configuration. The voltages generated by this process correspond to an inductance change of $\sim$0.1 μh under conditions of constant current.

When a sufficiently high rate of mass flow is injected, it can be seen that the arc voltage becomes constant. In Fig. 4, arc voltage becomes constant at a plenum pressure of $\approx$45 psi, corresponding to a mass flow rate of $\approx$12 g/sec. We identify this mass flow at constant arc voltage as $\dot{m}_c$. For $\dot{m} > \dot{m}_c$ there is no observable change in the constant value of arc voltage. The voltage-current plot (Fig. 5) is taken for $\dot{m} \geq \dot{m}_c$.

This voltage behavior strongly suggests that the arc adjusts the amount of mass to be processed through it. At low mass flow rates the arc "searches" for mass by blowing out into the tank. The arc may also erode the electrodes and insulator to acquire mass, but the total running time to date under $\dot{m} < \dot{m}_c$ conditions is too short to reach any definite conclusions. For $\dot{m} = \dot{m}_c$ the arc operates at constant voltage and current, and the energy absorbed by a changing inductance is negligible. For $\dot{m} > \dot{m}_c$ there is no change in V or I, suggesting that the arc bypasses a fraction of the mass flow.

Measured values of $\dot{m}_c$ are given in Fig. 6, plotted on the horizontal axis as flow rate at constant arc voltage. The vertical axis is a theoretical argon flow rate calculation, in which $\dot{m}$ is given by the expression due to Bennett et al.;[3] $(1/u_c)T$, where T is arc thrust, and u_c is the critical speed corresponding to the first ionization potential V_i. The importance of u_c is discussed in Pt. IV of this paper. For this arc the thrust is assumed to be due to the self-induced magnetic field, so that on the vertical axis of Fig. 6

$$\dot{m} = \tfrac{1}{2}\mu_0(h/b)I^2(m/2eV_i)^{1/2} = 3.3 \times 10^{-11} I^2 (\text{kg/sec}) \tag{4}$$

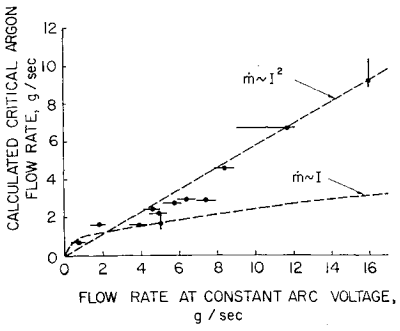

Fig. 6 Mass flow rate comparison plot. The vertical axis is a theoretical calculation for which $\dot{m} \sim I^2$ [Eq. (4)]. The horizontal axis is $\dot{m}_c$, the injected mass flow rate at which arc voltage is constant.

where h/b, the arc height to length ratio, is 0.46 when current flows to the whole electrode surface. The data do indeed follow an I^2 dependence, as shown by the straight line. A dependence $\dot{m} \sim I$ is plotted for reference. The experimental mass flow rates are all higher than those calculated from Eq. (4) by a factor of about 1.75, an error that is attributable to the approximations made in Eqs. (2) and (4).

Since by Eq. (4) $\dot{m}$ varies inversely as the critical speed u_c, the arc was run on helium, whose critical speed, $u_c = 3.43 \times 10^4$ m/sec, is 3.99 times that for argon. As was found for argon, the value of $\dot{m}_c$ for helium correlates reasonably well with Eq. (4). A voltage-current plot for helium, taken in the same manner as that for argon, is shown in Fig. 7. The impedance in helium is about 6.4 mΩ, compared to 2.0 mΩ for argon. At zero current, the intercept voltage V_0 is nearly the same for both gases, suggesting that V_0 is characteristic of the Elkonite electrode and not of the injected mass.

IV. Theory

There are thus two important experimental results. It is found that the arc has a constant impedance Z, and that the arc utilizes mass at a rate proportional to I^2. These results can be interpreted with the aid of the following simple model.

We approximate the rather complicated arc patterns by assuming a one-dimensional, constant area, steady plasma flow, accelerated from a uniform region where the magnetic field is $B = B_1$ to a uniform region where $B = B_2 = 0$. The fluid has only an x-velocity u, the magnetic field is in the positive z direction, and the electric field E and current density j are in the positive y-direction. Only x derivatives are nonzero. The plasma is treated as a continuous monofluid, with bulk properties of electrical conductivity σ, thermal conductivity κ and viscosity μ_f, all known functions of x.

The so-called "MHD approximations"[12] are assumed to be valid. Briefly, these approximations neglect displacement current, assume charge neutrality, and adopt vacuum values for μ and ϵ. The electric field transforms by $\mathbf{E}' = \mathbf{E} + \mathbf{v} \times \mathbf{B}$. Gravity and all external forces other than electromagnetic are neglected, as is radiation. The fluid is assumed to be nonionized in the uniform region upstream from the sheet.

The electrical conductivity σ is assumed to be a known function of x, and is zero in both the upstream and the downstream uniform regions. The condition of zero conductivity in the downstream region, (where $B_2 = 0$) is required by Ohm's Law, since $j_2 = 0$ only with $\sigma_2 = 0$. This condition results from the assumption of one-dimensionality, since in a one-dimensional geometry E must be constant by Maxwell's equation. In the two or three dimensional case, not considered here, E and B will go to zero at large x, and the condition $\sigma_2 = 0$ can be dispensed with.

Governing Equations

The flow is described by the following equations

Continuity

$$(d/dx)(\rho u) = 0 \tag{5}$$

Momentum

$$\rho u du/dx = -dp/dx + (d/dx)(\tfrac{4}{3}\,\mu_f du/dx) + jB \tag{6}$$

Energy

$$-(d/dx)(up) + (d/dx)(u\,\tfrac{4}{3}\,\mu_f du/dx) - (d/dx)(\rho u u^2/2) - (d/dx)[\rho u(C_v T + X)] + d/dx(\kappa dT/dx) + Ej = 0 \tag{7}$$

Maxwell's Equations

$$1)\quad dE/dx = 0 \tag{8}$$

$$2)\quad dB/dx = -\mu_0 j \tag{9}$$

Ohm's Law

$$j = \sigma(E - uB) \tag{10}$$

State

$$\frac{p}{\rho} = RT \tag{11}$$

The energy equation is derived from a form given by Pai,[14] where $C_v = 3/2\,k/m$, and X is the ionization energy. In this form the enthalpy is $h = [\gamma/(\gamma - 1)]T + X$, and the proper value of γ is $\frac{5}{3}$. It is assumed that in the arc the monofluid acquires an ionization energy corresponding to the first ionization potential, so that in the upstream fluid $X_1 = 0$, and downstream $X_2 = eV_i/m$, where m is the ion mass. Note that because of the simplified geometry, the Hall parameter does not appear in Ohm's Law.

First integrals can be readily obtained

$$\rho u = Q_0$$

$$E = E_0$$

Introducing these results in Eqs. (6) and (7) and eliminating j and T by using Eqs. (9) and (11)

$$Q_0 u + p + B^2/2\mu_0 - \tfrac{4}{3}\,\mu_f du/dx = K_0 \tag{12}$$

$$[\gamma/(\gamma - 1)]up + \tfrac{1}{2}Q_0 u^2 - \tfrac{4}{3}\,\mu_f u du/dx - \kappa(d/dx)(pu/RQ_0) + E_0 B/\mu_0 + Q_0 X = C_0 \tag{13}$$

Finally, introducing Eq. (9) in Eq. (10)

$$-(1/\mu_0)dB/dx = \sigma(E_0 - uB) \tag{14}$$

The three equations (12), (13), and (14) form a system of first-order differential equations in the variables, u, p, and B, with constants Q_0, E_0, K_0, and C_0. In addition, three boundary conditions are necessary;

$$\text{at } x = 0\text{: } B = B_1,\ du/dx = 0$$

$$\text{at } B = 0\text{: } du/dx = 0$$

corresponding to uniform upstream and downstream conditions, and given initial magnetic field.

The system of equations can in principle be solved, yielding a unique solution $u(x)$, $p(x)$, $B(x)$ for each set of values of the five constants Q_0, E_0, K_0, C_0, and B_1.

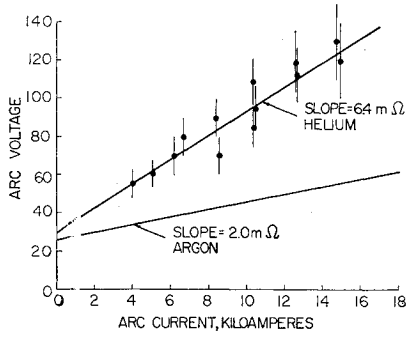

Fig. 7 Arc voltage vs current for helium flow rate $\dot{m} = \dot{m}_c$. Arc impedance is on the order of 6.4 mΩ.

Nondimensional Equations

The equations are nondimensionalized as follows:

$$u = u^*B_1^2/2\mu_0Q_0 \qquad K_0 = K_0^*B_1^2/2\mu_0$$
$$B = B^*B_1 \qquad C_0 = C_0^*B_1^4/(2\mu_0)^2Q_0$$
$$p = p^*B_1^2/2\mu_0 \qquad X = X^*B_1^4/(2\mu_0)^2Q_0^2$$
$$x = x^*\mu_f/Q_0 \qquad \sigma = \sigma^*2Q_0^2/\mu_fB_1^2$$
$$E = E^*B_1^3/2\mu_0Q_0 \qquad \kappa = \kappa^*R\mu_f$$

where it is assumed that μ_f is constant. We then obtain

$$u^* + p^* + B^{*2} - \tfrac{4}{3}\,du^*/dx^* = K_0^* \tag{12a}$$

$$(\gamma/\gamma - 1)u^*p^* + X^* + \tfrac{1}{2}\,u^{*2} - \tfrac{4}{3}\,u^*du^*/dx^* - \kappa^*du^*p^*/dx^* + 2E_0^*B^* = C_0^* \tag{13a}$$

$$-dB^*/dx^* = \alpha^*(E_0^* - u^*B^*) \tag{14a}$$

Downstream Conditions

The values of the nondimensional variables in the downstream region can be immediately related to the values of these variables in the upstream region, without considering the structure of the sheet. In regions 1 and 2 du/dx, dB/dx, and σ are zero, and while Eq. (14) becomes trivially satisfied, the other two become algebraic expressions.

In region 1 ($B^* = 1$, $X^* = 0$),

$$u_1^* + p_1^* + 1 = K_0^*$$
$$(\gamma/\gamma - 1)u_1^*p_1^* + \tfrac{1}{2}\,u_1^2 + 2E_0^* = C_0^* \tag{15}$$

which defines the constants K_0^* and C_0^* as a function of E_0^*, u_1^*, and p_1^*.

In region 2 ($B^* = 0$, $X^* = X_2^*$),

$$u_2^* + p_2^* = K_0^*$$
$$(\gamma/\gamma - 1)u_2^*p_2^* + \tfrac{1}{2}\,u_2^{*2} = C_0^* - X_2^*$$

which can be solved for u_2^* and p_2^*

$$u_2^* = \frac{\gamma K_0^*}{\gamma + 1}\left[1 \pm \left(1 - \frac{2(\gamma^2 - 1)(C_0^* - X_2^*)}{\gamma^2K_0^{*2}}\right)^{1/2}\right] \tag{16}$$

$$p_2^* = K_0^* - u_2^*$$

Also

$$M_2 = u_2^*/[\gamma u_2^*(K_0^* - u_2^*)]^{1/2} \tag{17}$$

Referring to Eq. (16), it can be seen that a necessary condition to have a solution for u_2^* is

$$2(\gamma^2 - 1)(C_0^* - X_2^*)/\gamma^2K_0^{*2} \leq 1 \tag{18}$$

Substituting from Eq. (15) gives

$$E_0^* \leq [\gamma^2/(4\gamma^2 - 1)]K_0^{*2} + \{X_2^*[\gamma/(\gamma - 1)]u_1^*p_1^* + \tfrac{1}{2}\,u_1^{*2}\}/2$$

There is thus an upper limit on the transverse electric field, designated by $E_{\max}^*$. Combining the equality of Eq. (18) with Eqs. (16) and (17), we find that for $E_0^* = E_{\max}^*$, the final Mach number M_2 is unity, so that this upper limit corresponds to choked flow. From Eq. (16), at sonic velocity $u_2^* = a_2^* = (\gamma/\gamma + 1)K_0^*$.

For $E_0^* < E_{\max}^*$, there are two possible final states. Since dM_2/du_2^* is always positive in the region of interest ($0 < u_2^* < K_0^*$), one state is subsonic and the other is supersonic. A detailed study of the arc structure, which will be presented in a later paper, shows that the supersonic final states are not attainable with any physically reasonable choice of the electrical conductivity function $\sigma(x)$. Only the subsonic or at most sonic final velocities are possible and the maximum attainable velocity is thus that of choked flow.

As remarked before, the downstream conditions will depend on five parameters Q_0, E_0, K_0, C_0, and B_1, or any combination of them such as Q_0, E_0, p_1, u_1, and B_1. In the experiments described herein, it appears that we can freely choose the pressure p_1 and velocity u_1 of the fluid injected, and the upstream magnetic field B_1. The first two are determined by the fast gas valve, while B_1, being induced by the discharge, depends on the total current I. Q_0 and E_0 cannot be freely chosen, since the arc adjusts the amount of mass to be accelerated (Q_0) and runs at a fixed potential (corresponding to E_0). Thus, in addition to the three free parameters p_1, u_1, and B_1, we must impose two additional physical constraints.

Among the various assumptions that could be made, the following appear particularly interesting: 1) the downstream flow (region 2) is sonic; and 2) the arc operates at a mass flow rate which minimizes the energy input from the external circuit.

Both of these have been made previously. Fay and Cochran[15] have assumed sonic downstream flow in a model of azimuthally nonuniform MPD arcs. Bennett et al.[3] postulate "by analogy with conventional arcs," that their discharge will attempt to operate at a mass flow which minimizes the input power.

To aid in discussing these assumptions, and applying them to the analysis, we will make some simplifications. For typical experimental conditions u_1^* and p_1^* can be neglected, giving $K_0^* \cong 1$. Thus, the choice of the sonic flow constraint uniquely determines E_0^* and u_2^*, independently of the other parameters. The minimum energy principle then determines Q_0. We will consider the minimum energy principle first.

The power input to the arc is

$$P = (\gamma/\gamma - 1)u_2p_2 + \tfrac{1}{2}\,Q_0u_2^2 + Q_0eV_i/m \tag{19}$$

Putting p_2 and u_2 in nondimensional form, differentiating Eq. (19) with respect to Q_0, and equating to zero, determines the flow at minimum power

$$Q_0 = (B_1^2/2\mu_0)/(2eV_i/m)^{1/2}(\gamma^2/\gamma^2 - 1)^{1/2} = \tfrac{5}{4}\,(B_1^2/2\mu_0u_c)$$

The final velocity and electric field in dimensional form for the case of minimum power are thus

$$u_2 = (\gamma^2 - 1)^{1/2}/(\gamma + 1)(2eV_i/m)^{1/2} = \tfrac{1}{2}u_c$$

and

$$E_0 = \tfrac{1}{2}\,[\gamma^2/(\gamma^2 - 1)]^{1/2}B_1(2eV_i/m)^{1/2} = \tfrac{5}{8}\,u_cB_1$$

E_0/B_1 and u_2 are therefore of the order of u_c, the critical speed for partially ionized plasmas discussed by Alfvén,[16] Fahleson,[17] and Lin.[18]

Note that the predicted dependencies on B_1 are $Q_0 \sim B_1^2$ and $E_0 \sim B_1$, in agreement with experiment.

Arc Impedance

For further comparison with the experiment, we express the previous results in terms of arc impedance. Setting the plasma voltage drop $V - V_0$ equal to E_0h, and arc current $I = bB_1/\mu_0$ from Ampere's Law, the impedance becomes

$$Z = (V - V_0)/I = \tfrac{5}{8}\,\mu_0(h/b)u_c \tag{20}$$

The calculated impedance for argon from Eq. (20) is 3.0 mΩ. This value of impedance is in reasonable agreement with the 2.0 mΩ impedance measured by experiment (Fig. 5).

In helium, where u_c is large, Eq. (20) gives an impedance of 12.0 mΩ, whereas the experimentally measured impedance is about 6.4 mΩ. This measured value is about 3.2 times that measured for argon, in fair agreement with the factor of 3.99 predicted by the ratio of critical speeds.

We may also crudely apply the one-dimensional model to the previous experiments discussed above with no mass injection.[8] If it is assumed that the accelerated mass is a mixture of doubly ionized copper and zinc electrode material, with u_c

$= 1.1 \times 10^4$ m/sec, then the theoretical impedance of this arc is ≈ 11.7 mΩ. This agreement with the measured value of 14 mΩ suggests that the arc without mass injection also accelerates ions to roughly the critical speed, so that the ion kinetic energy is small compared to the arc voltage of several hundred volts. This result also suggests that the electrode erosion rate is proportional to I^2.

V. Conclusions

Experimental results on a high current arc with argon and helium injection and no applied field show that the arc voltage stabilizes at a minimum mass flow $\dot{m}_c$, and that $\dot{m}_c$ varies as I^2. Furthermore, arc voltage increases linearly with current, corresponding to an arc impedance of approximately 2.0 $m\Omega$ for argon and 6.4 $m\Omega$ for helium.

A one-dimensional arc model is discussed, in which it is assumed that the downstream flow is sonic. The model also predicts a mass flow proportional to I^2, and a constant arc impedance, by invoking the minimum power principle. Both the mass flow and the impedance calculated from the model agree reasonably well with experimental values, despite the crudeness of the model. Impedance calculations applied to arcs with no mass injection show good agreement with experiment, suggesting that these arcs erode electrode material at a rate proportional to I^2.

References

[1] Ducati, A. D., Giannini, G. M., and Muehlberger, E., "Recent Progress in High Specific Impulse Thermoionic Acceleration," AIAA Paper 65-96, New York, 1965.

[2] John R. R., Bennett, S., and Connors, T., "Experimental Performance of a High Specific Impulse Arc Jet Engine," AIAA Paper 64-699, Philadelphia, 1964.

[3] Bennett, S., John R. R., Enos, G., and Tuchman, A., "Experimental Investigation of the MPD Arcjet," AIAA Paper 66-239, Monterey, Calif., 1966.

[4] Kruelle, G., "Characteristics and Local Analysis of MPD Thruster Operation," AIAA Paper 67-672, Colorado Springs, Colo., 1967.

[5] Blackstock, A. W., Fradkin, D. B., Roehling, D. T., and Stratton, T. F., "A Cesium Magnetohydrodynamic Coaxial Arc Jet," Rept. 3735, 1967, Los Alamos Scientific Lab., Los Alamos, N. Mex.

[6] Moore, R. A., Cann, G. L., and Gallagher, L. R., "High Specific Impulse Arc Jet Thrustor Technology," Phase I Final Rept. 5090, 1965, Electro Optical Systems, Pasadena, Calif.

[7] Stratton, T. F., "High-Current Steady-State Coaxial Plasma Accelerators," *AIAA Journal*, Vol. 3, No. 10, Oct. 1965, pp. 1961–1963.

[8] Burton, R. L. and Chang, O. Y-S., "Acceleration Process in a Stabilized High-Current Arc," *AIAA Journal*, Vol. 6, No. 11, Nov. 1968, pp. 2190–2192.

[9] Eckbreth, A. C., Clark, K. E., and Jahn, R. G., "Current Pattern Stabilization in Pulsed Plasma Accelerators," *AIAA Journal*, Vol. 6, No. 11, Nov. 1968, pp. 2125–2132.

[10] Lowder, R. S. and Hoh, F. C., "Fast Gas Valve for Plasma Research," *Review of Scientific Instruments*, Vol. 33, No. 11, Nov. 1962, pp. 1236–1238.

[11] Black, N. A., "Dynamics of a Pinch Discharge Driven by a High Current Pulse Forming Network," Rept. 778, 1966, Princeton Univ., Princeton, N. J.

[12] Hughes, W. F. and Young, F. T., *The Electromagnetodynamics of Fluids*, Wiley, New York, 1966.

[13] Jahn, R. G., *Physics of Electric Propulsion*, McGraw-Hill, 1968, Chap. 8.

[14] Pai, S-I., "Energy Equation of Magneto-Gas Dynamics," *Physical Review*, Vol. 105, No. 5, March 1957, pp. 1424–1426.

[15] Fay, T. A. and Cochran, R. A., "An Actuator-disc Model for Azimuthally Non-uniform MPD Arcs," AIAA Paper 68-714, Los Angeles, Calif., 1968.

[16] Alfvén, H., "Collision Between a Non-ionized Gas and a Magnetized Plasma," *Review of Modern Physics*, Vol. 32, No. 4, Oct. 1960, p. 710.

[17] Fahleson, U. V., "Experiments with Plasma Moving Through Neutral Gas," *Physics of Fluids*, Vol. 4, 1961, pp. 123–127.

[18] Lin, S. C., "Limiting Velocity for a Rotating Plasma," *Physics of Fluids*, Vol. 4, No. 10, Oct. 1961, pp. 1277–1288.